Molecular Microbiology (2003) **48**(4), 977–988

Evidence that acetyl phosphate functions as a global signal during biofilm development

Alan J. Wolfe,[1,2*] Dong-Eun Chang,[3] Jason D. Walker,[4] Jeanine E. Seitz-Partridge,[2] Michael D. Vidaurri,[1,3] Charles F. Lange,[1] Birgit M. Prüß,[5] Margaret C. Henk,[4] John C. Larkin[4] and Tyrrell Conway[3]

[1]*Department of Microbiology and Immunology,*
[2]*Molecular Biology Program, Stritch School of Medicine, Loyola University Chicago, Maywood, IL 60153, USA.*
[3]*Department of Botany and Microbiology, University of Oklahoma, Norman, OK 73069, USA.*
[4]*Department of Biological Sciences, Louisiana State University, Baton Rouge, LA 70803, USA.*
[5]*Department of Microbiology and Immunology, University of Illinois at Chicago, Chicago, IL 60612, USA.*

Summary

We used DNA macroarray analysis to identify genes that respond to the status of the intracellular acetyl phosphate (acP) pool. Genes whose expression correlated negatively with the ability to synthesize acP (i.e. negatively regulated genes) function primarily in flagella biosynthesis, a result consistent with observations that we published previously (Prüß and Wolfe, 1994, *Mol Microbiol* 12: 973–984). In contrast, genes whose expression correlated positively with the ability to synthesize acP (i.e. positively regulated genes) include those for type 1 pilus assembly, colanic acid (capsule) biosynthesis and certain stress effectors. To our knowledge, this constitutes the first report that these genes may respond to the status of the intracellular acP pool. Previously, other researchers have implicated flagella, type 1 pili, capsule and diverse stress effectors in the formation of biofilms. We therefore tested whether cells altered in their ability to metabolize acP could construct normal biofilms, and found that they could not. Cells defective for the production of acP and cells defective for the degradation of acP could both form biofilms, but these biofilms exhibited characteristics substantially different from each other and from biofilms formed by their wild-type parent. We confirmed the role of individual cell surface structures, the expression of which appears to correlate with acP levels, in *fim* or *fli* mutants that cannot assemble type 1 pili or flagella respectively. Thus, the information gained by expression profiling of cells with altered acP metabolism indicates that acP may help to co-ordinate the expression of surface structures and cellular processes involved in the initial stages of wild-type biofilm development.

Accepted 3 January, 2003. *For correspondence. E-mail awolfe@lumc.edu; Tel. (+1) 708 216 5814; Fax (+1) 708 216 9574.

Introduction

Some bacteria form complex, sessile communities called biofilms that begin to develop when bacteria transit from a free-living, planktonic existence to a lifestyle in which they attach firmly to surfaces, interfaces and/or each other. This transition involves reversible adsorption of planktonic cells to a suitable surface often facilitated by flagella, followed by irreversible attachment and colonization, most often facilitated by pili and other adhesins. After the formation of an attached monolayer, three-dimensional structures develop. These structures comprise water-filled channels that separate mushroom-shaped microcolonies composed of cells and their products encased in a matrix of extracellular polysaccharides, also known as capsule (Stoodley *et al.*, 2002).

Cells co-ordinate gene expression in response to environmental cues via a select subset of small molecules, including ppGpp, cAMP and leucine (Barker *et al.*, 2001a,b; Bruckner and Titgemeyer, 2002; Chang *et al.*, 2002; Hung *et al.*, 2002). Several years ago, Wanner and others proposed that acetyl phosphate (acP), a high-energy, phosphorylated, activated acetate derivative, also plays a global regulatory role (Wanner and Wilmes-Riesenberg, 1992; McCleary *et al.*, 1993). Yet, in contrast to most of its counterparts, the manner in which acP might function as a global signal remains an enigma.

Given its central location within carbon metabolism, acP is well suited to monitor nutritional status, a contention supported by the fact that acP levels respond to the quantity and quality of the nutritional environment (McCleary and Stock, 1994; Prüß and Wolfe, 1994). As the intermediate of the phosphotransacetylase–acetate kinase (Pta-AckA) pathway (Fig. 1) (Rose *et al.*, 1954; Brown *et al.*, 1977), acP plays a critical role during aerobic growth on excess carbon and during mixed acid fermentation. In the presence of oxygen, when the carbon

flux into cells exceeds the amphibolic capacity of the tricarboxylic acid (TCA) cycle, cells recycle coenzyme A (CoASH) by directing excess acetyl-coenzyme A (acCoA) through the Pta-AckA pathway, excreting acetate and generating ATP (Brown *et al*., 1977; Chang *et al*., 1999). In the absence of oxygen, acCoA cannot enter the TCA cycle. To regenerate CoASH, the cells guide acCoA through the Pta-AckA pathway, again excreting acetate while generating ATP (el-Mansi and Holms, 1989). As a result, acP levels can reflect the nutritional status of the cell: a large acP concentration reflects either the presence of excess carbon and/or the lack of oxygen, whereas a small concentration reflects limited carbon in the presence of oxygen.

Here, we present evidence that the status of the intracellular acP pool affects the expression of flagella, type 1 pili, colanic acid and certain stress effector genes and influences the ability of *Escherichia coli* cells to form biofilms.

Results

Identification of acP-responsive genes

To identify genes that respond to acP, we used DNA macroarrays to compare *E. coli* wild-type cells (strain AJW678) with cells lacking AckA (*ackA* mutant; strain AJW1939) or both Pta and AckA (*pta ackA* double mutant; strain AJW2013). Cells that lack AckA can convert acCoA to acP but cannot degrade acP to acetate efficiently (Fig. 1). Therefore, these cells accumulate acP to a higher level than do wild-type cells, especially when grown on a carbon source that feeds into the bottom half of the glycolytic pathway (e.g. serine present in tryptone). In contrast, cells that lack Pta and AckA do not synthesize acP from either acCoA or acetate (Fig. 1) (McCleary and Stock, 1994; Prüß and Wolfe, 1994). The extracellular

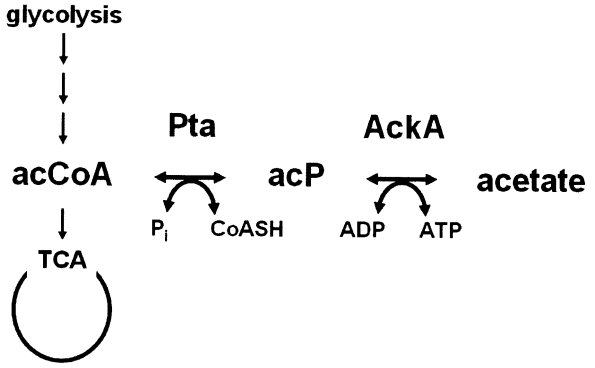

Fig. 1. Schematic of the phosphotransacetylase (Pta)–acetate kinase (AckA) pathway that converts acetyl-coenzyme A (acCoA) to acetate via an acetyl phosphate (acP) intermediate. P_i, inorganic phosphate; CoASH, coenzyme A; TCA, tricarboxylic acid cycle.

acetate concentrations and intracellular acCoA and acP concentrations associated with the single *pta* mutant resemble those of the double *pta ackA* mutant (Prüß and Wolfe, 1994). Thus, we chose the double mutant over the single mutant to avoid AckA-dependent activation to acP of any trace quantities of acetate that may be generated by non-Pta-dependent mechanisms.

We aerated cells in tryptone broth (TB) at 37°C. Wild-type cells grew about 40% more rapidly (doubling time = 32 min) than either of the mutants. However, the mutants doubled at almost identical rates (44 and 46 min respectively). Wild-type cells evolved ammonia and consumed amino acids in the following preferential order: L-serine, L-aspartate, L-tryptophan, L-glutamate, L-threonine, L-alanine, as reported previously (Prüß *et al*., 1994). Both mutants evolved ammonia and consumed amino acids preferentially in a manner that resembled that of wild-type cells, but with some significant differences: most notably, slower rates of consumption for tryptophan, glutamate and threonine. However, both mutants consumed amino acids in the same order at comparable rates and evolved ammonia similarly (data not shown). These similar behaviours gave us confidence to compare the *ackA* and *pta ackA* mutants directly.

We harvested cells during early exponential growth (A_{590} = 0.1), when acP levels peak in wild-type cells (Prüß and Wolfe, 1994). We purified the RNA, generated cDNA, hybridized a paired set of macroarrays (Sigma-GenoSys) and, for each sample, analysed and processed the data as described previously (Conway *et al*., 2002). We normalized the data by expressing the intensity of each gene-specific spot as a percentage of the sum of spot intensities, calculated the ratio of gene expression for each mutant relative to the control expression level (wild-type) and used Student's *t*-test to determine the probability that the ratio is significant (*P*-value). Our statistical analysis established significantly regulated genes meeting two criteria: ratio values ≥2.5 standard deviations from the mean of the log ratios (99% confidence) with *P*-values ≤0.05 (95% probability). A total of 146 genes [≈ 3.5% of 4290 total open reading frames (ORFs) identified in *E. coli*] met these criteria. We performed subsequent analyses only on this subset of genes.

To distinguish genes that respond to the status of acP from those that respond to a slower rate of growth or to a general defect in acetate excretion, we plotted the $\log_{10}$ of the expression ratio *pta ackA*/WT against the $\log_{10}$ of the expression ratio *ackA*/WT (Fig. 2A). Using this strategy, genes that respond identically in both mutants when compared with their wild-type parent map to a line with a slope of 1 and a *y*-intercept of 0. Presumably, such genes respond either to a slower rate of growth or to a general defect in the Pta-AckA pathway, e.g. the accumulation of the pathway substrate (acCoA) or the absence of its prod-

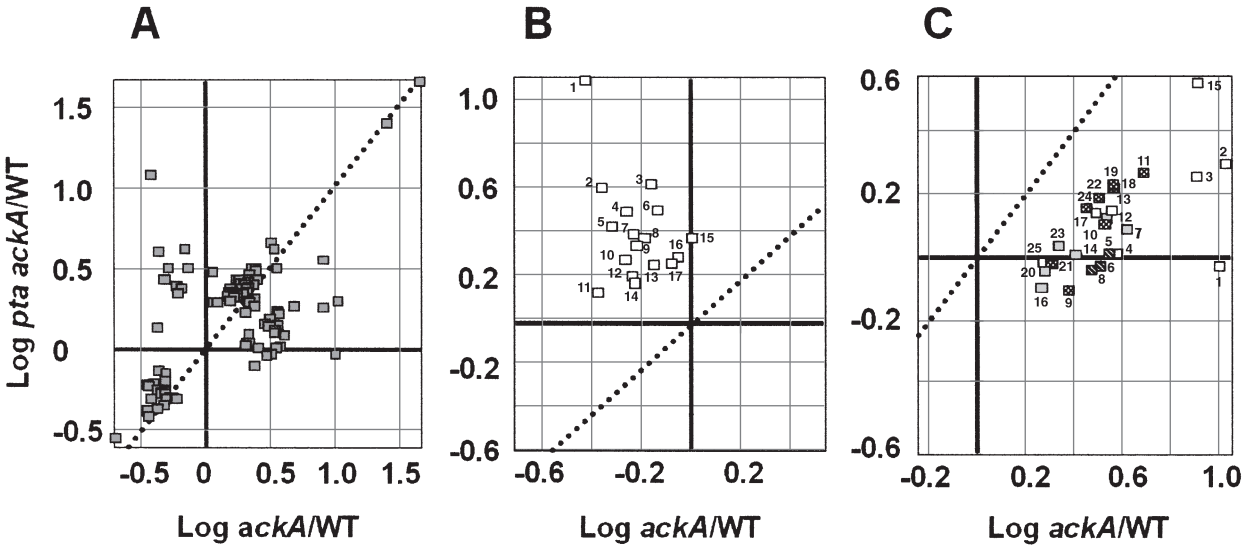

Fig. 2. Scatter plots displaying genes significantly overexpressed or underexpressed relative to wild-type cells (AJW678) by mutant cells defective for *pta ackA* (AJW2013) or *ackA* (AJW1939). Cells were aerated in TB at 37°C, harvested at A_{590} = 0.1 and subjected to DNA macroarray analysis. The dotted line ($m = 1$, $b = 0$) represents the predicted position of genes identically expressed in cells of both mutants.
A. All genes that are expressed differentially.
B. Of the genes shown in (A), only those negatively influenced by acP are shown. Numbers refer to those in Table 1.
C. Of the genes shown in (A), only those positively influenced by acP are shown. Open squares, genes involved in stress responses. Chequered squares, genes involved in type I pilus biosynthesis and assembly. Cross-hatched squares, genes involved in capsule biosynthesis. Grey squares, hypothetical genes and those of putative function. Numbers refer to those in Table 2.

uct (acetate). In contrast, genes that respond negatively to acP levels map above and to the left of the line, whereas those that respond positively to acP map below and to the right of that line.

Under the experimental conditions tested, 50 genes appeared to respond negatively to high acP levels; those that responded most significantly (≥5 SD) function exclusively in flagellar biosynthesis and assembly (Fig. 2B, Table 1). These include genes involved in assembly of the filament and hook (*fliC*, *flgE*, *fliD*, *flgK*, *flgD*, *flgL*), the basal body (*flgC*, *flgB*, *flgG*, *flgA*, *flgF*, *fliL*, *flgJ*), the switching mechanism (*fliM*), the chemotactic signal trans-

Table 1. Genes significantly upregulated in a *pta ackA* mutant compared with an *ackA* mutant.[ab]

			pta ackA/*ackA*		*pta ackA*/WT		*ackA*/WT		
	Gene	b no.	Ratio	Log_{10}	Ratio	Log_{10}	Ratio	Log_{10}	Gene product
1	*fliC*	1923	30.9	1.5	11.8	1.1	–2.6	–0.4	Flagellin, major filament component
2	*flgE*	1076	8.9	1.0	4.0	0.6	–2.3	–0.4	Hook
3	*fliD*	1924	5.8	0.8	4.1	0.6	–1.4	–0.2	Filament cap
4	*flgC*	1074	5.5	0.7	3.1	0.5	–1.8	–0.3	Basal body-rod
5	*flgB*	1073	5.4	0.7	2.6	0.4	–2.1	–0.3	Basal body-rod
6	*flgK*	1082	4.1	0.6	3.2	0.5	–1.3	–0.1	Hook–filament junction
7	*flgG*	1078	4.1	0.6	2.5	0.4	–1.7	–0.2	Basal body-rod
8	*flgD*	1075	3.6	0.6	2.2	0.3	–1.6	–0.2	Hook assembly initiation
9	*flgL*	1083	3.4	0.5	2.4	0.4	–1.4	–0.2	Hook–filament junction
10	*fliA*	1922	3.4	0.5	1.9	0.3	–1.8	–0.3	Flagellar-specific sigma factor
11	*fliL*	1944	3.1	0.5	1.4	0.1	–2.3	–0.4	Basal body-rod
12	*flgA*	1072	2.7	0.4	1.6	0.2	–1.7	–0.2	Basal body assembly
13	*flgF*	1077	2.5	0.4	1.8	0.3	–1.4	–0.1	Basal body-rod
14	*fliM*	1945	2.5	0.4	1.5	0.2	–1.7	–0.2	Motor switch; energy transduction
15	*cheY*	1882	2.3	0.4	2.3	0.4	1.0	0	Chemotactic signalling
16	*tar*	1886	2.2	0.3	1.9	0.3	–1.1	–0.1	Chemoreceptor
17	*flgJ*	1801	2.1	0.3	1.8	0.3	–1.2	–0.1	Basal body-rod

a. Numbers refer to those in Fig. 2B.
b. Significance determined as having a ratio ≥5 SD from the mean of the ratios and having a *P*-value ≤0.05. Another 33 genes not listed exhibited a significant ratio between 2.5 and 5 SD from the mean of the ratios and had a *P*-value ≤0.05.

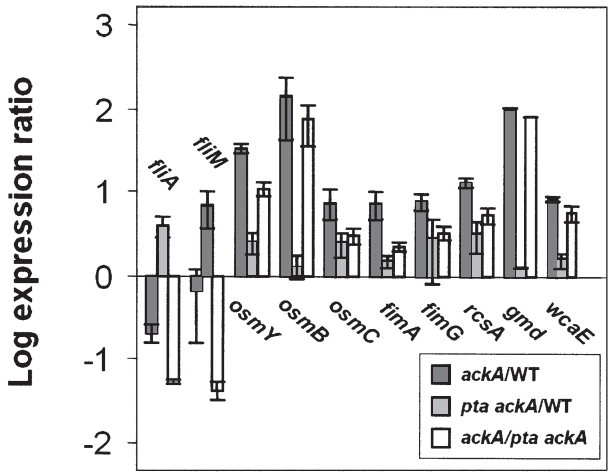

Fig. 3. Mean log expression ratios ± SEM of a subset of genes. Cells were aerated in TB at 37°C, harvested at A_{590} = 0.1 and subjected to quantitative RT-PCR.

duction pathway (*cheY*, *tar*) and transcription of those genes (*fliA*). We confirmed these results, using quantitative reverse transcription polymerase chain reaction (RT-PCR) to analyse *fliA* and *fliM* (Fig. 3). Both genes were expressed at highest levels in the *pta ackA* mutant, followed by the wild type and then the *ackA* mutant, consistent with the array results. Other flagellar genes responded significantly, but to a lesser degree (≥2.5 SD): they include those involved in hook length control (*fliK*), flagellar-specific export (*flgN*, *flhB*, *fliI*, *fliJ*), chemotactic signalling and energy transduction (*cheB*, *cheZ*, *cheR*, *trg*, *motB*), regulation (*flhD*, *flhC*) and unknown functions (*fliY*, *fliZ*). Non-flagellar genes that responded negatively to high acP levels encode outer membrane porins (*ompF*, *ompC*), other proteins associated with or predicted to associate with the envelope (*rbsB*, *b1966*, *yqiH*, *glpD*, *rfbX*, *rbsD*), chaperones (*dnaK*, *mopB*, *mopA*), the regulators of the maltose regulon (*malT*) and the carnitine operon (*caiF*) and an enzyme involved in carnitine metabolism (*caiD*) (data not shown, see http://www.ou.edu/microarray).

In contrast, 46 genes appeared to respond positively to high acP concentrations; the most significant (≥4.8 SD) function primarily in stress protection (*osmB*, *ivy*, *osmY*, *osmC*, *dps*, *hslJ*), colanic acid biosynthesis (*rcsA*, *wcaE*, *gmd*), type 1 pilus assembly (*fimG*, *fimI*, *fimA*, *fimC*, *fimH*, *fimF*) and the assembly of putative non-type 1 pili (*b0943*, *sfmC*) (Fig. 2C, Table 2). We confirmed these results, using quantitative RT-PCR to analyse *osmY*, *osmB*, *osmC*, *fimA*, *fimG*, *rcsA*, *gmd* and *wcaE* (Fig. 3). These genes were expressed at highest levels in the *ackA* mutant, followed by the *pta ackA* mutant and then by the

Table 2. Genes significantly upregulated in an *ackA* mutant compared with a *pta ackA* mutant.[ab]

			pta ackA/*ackA*		*pta ackA*/WT		*ackA*/WT		
	Gene	b no.	Ratio	Log_{10}	Ratio	Log_{10}	Ratio	Log_{10}	Gene product
1	*osmB*	1283	–10.9	–1.0	–1.1	<–0.05	10.1	1.0	Osmotically inducible lipoprotein
2	*ivy*	0220	–5.5	–0.7	2.0	0.3	10.8	1.0	Inhibitor of vertebrate lysozyme, previously *yfkE*
3	*osmY*	4376	–4.6	–0.7	1.8	0.3	8.2	0.9	Hyperosmotically inducible periplasmic protein
4	*yjbE*	4026	–3.6	–0.6	1.0	<0.05	3.6	0.6	Hypothetical protein
5	*rcsA*	1951	–3.5	–0.6	1.0	<0.05	3.6	0.6	Colanic acid biosynthesis (CAB), positive regulator
6	*wcaE*	2055	–3.5	–0.5	–1.1	<–0.05	3.3	0.5	CAB, putative glycosyl transferase
7	*yafP*	0234	–3.4	–0.5	1.2	0.1	4.1	0.6	Hypothetical protein
8	*gmd*	2053	–3.4	–0.5	–1.1	–0.1	3.0	0.5	CAB, GDP-D-mannose dehydratase
9	*b0943*	0943	–3.0	–0.5	–1.3	0.1	2.4	0.4	Putative fimbrial protein
10	*sfmC*	0531	–2.7	–0.4	1.3	0.1	3.4	0.5	Putative fimbrial chaperone
11	*fimG*	4319	–2.7	–0.4	1.8	0.3	4.9	0.7	Type 1 pilus, morphology
12	*b1172*	1172	–2.6	–0.4	1.3	0.1	3.5	0.5	Hypothetical protein
13	*osmC*	1482	–2.6	–0.4	1.4	0.1	3.7	0.6	Osmotically inducible protein
14	*ycfJ*	1110	–2.4	–0.4	1.0	<0.05	2.6	0.4	Hypothetical protein
15	*dps*	0812	–2.3	–0.4	3.5	0.6	8.3	0.9	Starvation, global regulator
16	*yiaD*	3552	–2.3	–0.4	–1.3	–0.1	1.9	0.3	Putative outer membrane protein
17	*hslJ*	1379	–2.3	–0.4	1.4	0.1	3.1	0.5	Heat shock protein
18	*fimI*	4315	–2.3	–0.4	1.6	0.2	3.7	0.6	Type 1 pilus, minor protein
19	*fimA*	4314	–2.2	–0.3	1.7	0.2	3.7	0.6	Type 1 pilus, major subunit, pilin
20	*ybdG*	0577	–2.2	–0.3	–1.1	<–0.05	1.9	0.3	Putative transport protein
21	*fimC*	4316	–2.1	–0.3	–1.1	<–0.05	2.0	0.3	Type 1 pilus, periplasmic chaperone
22	*fimH*	4320	–2.1	–0.3	1.5	0.2	3.2	0.5	Type 1 pilus, D-mannose-specific adhesin
23	*b2833*	2833	–2.1	–0.3	1.1	<0.05	2.2	0.3	Hypothetical protein
24	*fimF*	4318	–2.0	–0.3	1.4	0.2	2.9	0.5	Type 1 pilus, morphology
25	*eco*	2209	–2.0	–0.3	–1.1	<–0.05	1.9	0.3	Ecotin, serine protease inhibitor

a. Numbers refer to those in Fig. 2C.
b. Significance determined as having a ratio ≥4.8 SD from the mean of the ratios and having a *P*-value ≤0.05. Another 21 genes not listed exhibited a significant ratio between 2.5 and 4.8 SD from the mean of the ratios and had a *P*-value ≤0.05.

wild-type parent, consistent with the array results. Apparently, these genes respond not only to acP but also, to a lesser degree, to slowed growth or a general pathway defect. Other genes responded significantly, but to a lesser degree (≥2.5 SD): among these are two other genes involved in colanic acid biosynthesis (*wcaD*, *ugd*) and one of unknown function located within the colanic acid biosynthetic locus (*orf1.3*); also included are genes that encode an outer membrane protein (*ompX*), a putative regulator of maltose metabolism (*sfsA*), a component of formate dehydrogenase-H (*fdhF*) and glutathione oxidoreductase (*gor*) (data not shown, see http://www.ou.edu/microarray).

Twenty-seven genes appeared to respond positively to a slower growth rate or a general pathway defect; these genes function primarily in stress protection and the TCA cycle (Fig. 2A, see http://www.ou.edu/microarray). In contrast, 23 genes responded negatively; most remain hypothetical or putative, whereas others do not fall into clearly delineated functional categories (Fig. 2A, see http://www.ou.edu/microarray).

These results agree with our previous report that *pta ackA* mutants synthesize far more flagella than *ackA* mutants (Prüß and Wolfe, 1994). As predicted from our array data, *ackA* mutants produced mucoid colonies. In contrast, wild-type cells and *pta ackA* mutants produced non-mucoid colonies (Fig. 4A). Also as predicted, *ackA* mutants exhibited numerous pili, as do wild-type cells. In contrast, *pta ackA* mutants displayed few pili (Fig. 4B). At first glance, it might be puzzling that *pta ackA* mutants display substantially fewer pili than wild-type cells. Like *ackA* mutants, *pta ackA* mutants express all the *fim* structural genes (*fimAIFGH*) at higher levels than wild-type cells (Table 2, Fig. 2C). We suspect the difference lies with the behaviour of *fimC*, which encodes the type 1 pilus-specific chaperone that delivers pilus subunits to the pilus-specific usher, an assembly platform encoded by *fimD* (Sauer *et al*., 2000). Unlike *ackA* mutants, *pta ackA* cells apparently do not upregulate *fimC* (Table 2, Figs 2C and 5). This result leads us to suspect that an excess of pilus subunits might overload the FimC chaperone and that this overload results in reduced pilus assembly. If so, we do not suspect the usher, FimD, because both *ackA* and *pta ackA* mutants appear to express similar amounts of *fimD* (Fig. 5). Regardless of the underlying mechanism responsible for the *pta ackA* pilus assembly defect, taken together, our results support the argument that high acP levels enhance colanic acid production and type 1 pilus assembly, whereas low acP levels favour flagellar expression.

Pellicle and abiotic surface-adherent biofilm formation

Escherichia coli cells can simultaneously form two different structured communities during growth in static culture: a pellicle that forms on the surface of the culture medium and an abiotic surface-adherent biofilm that forms at the air–liquid interface. Formation of the pellicle depends, in part, upon the presence of intact type 1 pili that permit cell–cell interactions (Harris *et al*., 1990). As others have previously implicated type 1 pili and other adhesins, flagella, colanic acid and several stress responses in the formation of surface-adherent biofilms (reviewed by Stoodley *et al*., 2002), we compared the pellicle- and surface-adherent biofilm-forming ability of wild-type cells with that of cells that either accumulate acP (*ackA*) or do not synthesize it (*pta ackA*). For these experiments, we grew cells at 37°C in static TB cultures. At 2 h intervals, we monitored the A_{590} as a measure of biomass. Wild-type cells grew more rapidly (doubling time = 56 min) than either of the mutants. The mutants, however, doubled at identical rates (doubling time = 121 min). Wild-type cells

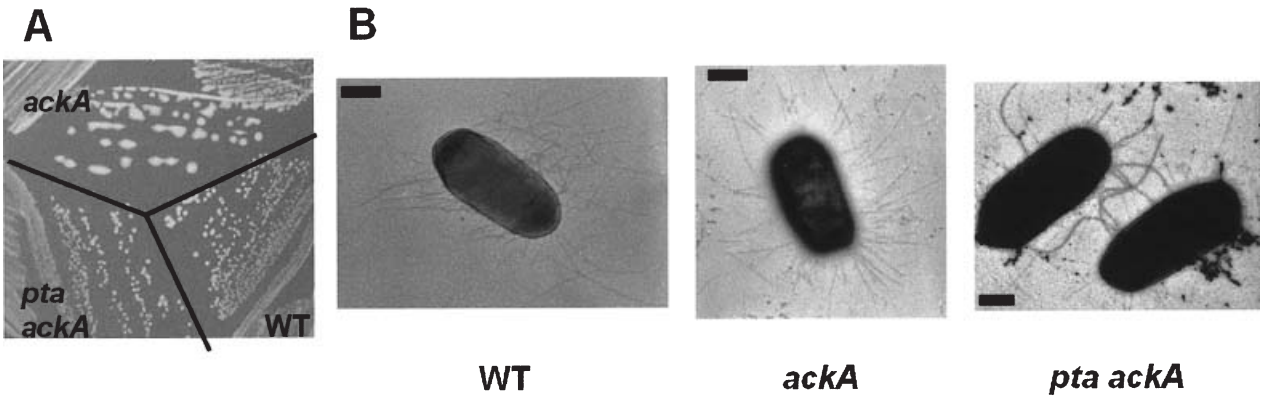

Fig. 4. A. Mucoidy phenotype of colonies formed by cells wild type (AJW678) or deficient for either *ack* (AJW1939) or *pta* and *ackA* (AJW2013). Cells were grown at 37°C on defined medium (M63) supplemented with 0.2% glucose.
B. Transmission electron micrographs of wild-type cells (AJW678), *ackA* mutant cells (AJW1939) or *pta ackA* mutant cells (AJW2013) grown at 37°C in TB and harvested at A_{590} = 0.4. Each bar represents 1 μm.

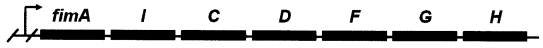

P/A	-0.3	-0.4	-0.3	NS	-0.3	-0.4	-0.3
P/+	0.2	0.2	NS	NS	0.2	0.3	0.2
A/+	0.6	0.6	0.3	NS	0.5	0.7	0.5

Fig. 5. Schematic showing expression profiles of the *fim* operon. P/A, $\log_{10}$(*pta ackA/ackA*); P/+, $\log_{10}$(*pta ackA*/WT); A/+, $\log_{10}$(*ackA*/WT). NS, not significantly different.

consumed amino acids and evolved ammonia in a manner that resembles that observed under aerated conditions (data not shown). Although they did so more slowly than their wild-type parent, both mutants consumed amino acids and evolved ammonia similarly (data not shown). Biofilm development requires growth through exponential phase (Danese *et al.*, 2001). Thus, the difference between wild-type and mutant growth rates may make direct comparison between wild-type and mutant biofilm development problematic. However, the virtually identical rates of growth and ammonia evolution and the similar profiles of amino acid consumption exhibited by the mutants permits their direct comparison.

To observe the ability of each strain to form a surface-adherent biofilm at the liquid–air interface, we stained 18 h cultures with crystal violet, and rinsed away non-adherent cells (Fig. 6A). The morphology of each biofilm appeared to be distinctly different. Both wild-type and *pta ackA* mutant cells produced substantial surface-adherent biofilms in contrast to *ackA* mutant cells, which constructed a sparse biofilm. To examine these biofilms more closely, we performed differential interference contrast (DIC) microscopy on biofilms grown on thin strips of microscope slides (Fig. 6B). After 6 h incubation, wild-type cells produced large microcolonies. In contrast, *pta ackA* mutants formed smaller microcolonies, whereas *ackA* mutants formed even smaller ones.

The morphology of each pellicle also appeared to be distinctly different. Wild-type cells formed a film-like pellicle that covered the entire surface of the static culture (Fig. 6C). Upon this film, complex swirls of colony-like structures formed. When vortexed, the wild-type pellicle did not disperse easily; instead, it formed tight aggregates (data not shown). In contrast, *ackA* mutant cells formed isolated rafts of cells. When vortexed, these cells also formed aggregates (data not shown). Like wild-type cells, *pta ackA* mutant cells formed a film that covered the entire surface of the culture. In contrast to wild-type and *ackA* mutant pellicles, *pta ackA* mutant cells formed few colony-like structures and dispersed easily into a homogeneous suspension when vortexed (data not shown).

Finally, we began to explore the molecular basis that underlies the distinct characteristics displayed by biofilms and pellicles formed by *ackA* and *pta ackA* mutants. We introduced a mutant allele (*fliA*) that precludes the expression of flagella into cells either wild type or deficient for *ackA* alone or both *pta* and *ackA*. As reported previously (Pratt and Kolter, 1998), the lack of flagella eliminated the ability of otherwise wild-type cells (*fliA*) to form a biofilm (Table 3). Similarly, *pta ackA* mutants that cannot synthesize flagella (*pta ackA fliA*) formed, at best, very poor biofilms. In contrast, *ackA fliA* mutants formed biofilms indistinguishable from those produced by their *ackA fliA*$^+$ parent. Thus, biofilm formation by the *ackA* mutant does not require flagella.

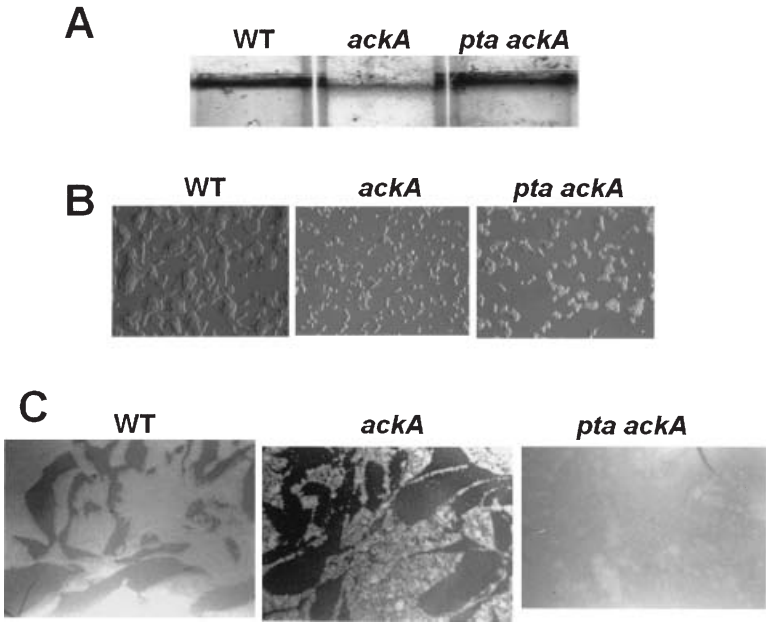

Fig. 6. A. Surface-adherent biofilms formed by cells wild-type (WT) or deficient for either *ackA* or *pta ackA*. Cells were grown without aeration at 37°C in TB. After 18 h incubation, the triplicate cultures were stained with crystal violet, the non-adherent cells were rinsed away, and the adherent cells that formed a biofilm at the air–liquid interface were visualized using an Alphaimager 2000 documentation and analysis system. Representative images are shown.
B. DIC micrographs of microcolonies formed by wild-type cells (AJW678), *ackA* mutant cells (AJW1939) or *pta ackA* mutant cells (AJW2013). Duplicate cultures were grown without aeration for 6 h at 37°C on thin strips of microscope slides partially immersed in TB. Representative images are shown.
C. Pellicles formed by cells wild type (AJW678) or defective for either *ackA* (AJW1939) or *pta ackA* (AJW2013). Cells were grown without aeration at 37°C in TB. After 18 h incubation, the triplicate cultures were photographed using a Wild dissecting microscope at a magnification of 25×. Representative images are shown. Note cracks at the bottom left of the wild-type pellicle and the upper right of the *pta ackA* pellicle.

Table 3. Biofilm phenotypes.

Strain	Relevant genotype	Phenotype[a]
AJW678	Wild type	Wild-type standard
AJW1939	*ackA*::Km	*ackA* standard
AJW2067	*ackA*::Tn*phoA′*-2	*ackA* standard
AJW2013	Δ(*ackA pta hisJ hisP dhu*)	*pta ackA* standard
AJW2145	*fliA*::Tn5	0
AJW2149	*ackA*::Km *fliA*::Tn*5*	*ackA* standard
AJW2153	Δ(*ackA pta hisJ hisP dhu*) *fliA*::Tn*5*	Trace
AJW2063	Δ*fimA*::Km	0
AJW2070	*ackA*::Tn*phoA′*-2 Δ*fimA*::Km	0
AJW2064	Δ(*ackA pta hisJ hisP dhu*) Δ*fimA*::Km	0
AJW2061	*fimH*::Km	0
AJW2069	*ackA*::Tn*phoA′*-2 *fimH*::Km	0
AJW2062	Δ(*ackA pta hisJ hisP dhu*) *fimH*::Km	0

a. For images of phenotypes, see Fig. 6.
0, no biofilm.

The tendency of wild-type and *ackA* mutant biofilms to resist dispersal by agitation correlates well with their expression of numerous pili, surface structures intimately involved in cell–cell contact. In contrast, the easy dispersal of *pta ackA* mutant biofilms reflects their relative lack of pili. Both mannose and its analogue methyl-α-D-mannopyranoside inhibit wild-type pellicle formation by binding a D-mannose-specific adhesin, encoded by *fimH* and used for cell–cell contact (Harris *et al*., 1990). Both inhibitors interfered with the formation of wild-type and *ackA* mutant pellicles and surface-adherent biofilms (Table 4), but not with those formed by *pta ackA* mutants. However, when we introduced mutant alleles that eliminate the expression of the entire type 1 pilus (*Δfim*) or simply the adhesin (*fimH*), cells formed neither pellicles nor surface-adherent biofilms, regardless of the status of *ackA* and/or *pta* (Table 3). Taken together, our observations suggest that type 1 pili must play some important role in biofilm development by *pta ackA* mutants, but that the small number they exhibit cannot resist dispersal.

Table 4. Effect of mannose and a mannose analogue on pellicle formation.[a]

Strain	Mannose pellicle	Mannose SA	MADMP pellicle	MADMP SA
Wild type	17.5 (A)	17.5 (A)	20 (B)	50 (A)
ackA	17.5 (A)	ND	20 (A)	30 (A)
pta ackA	>100	>100	>100	>100

a. Cells were grown in TB at 37°C in the absence or presence of mannose or methyl-α-D-mannopyranoside (MADMP) across a range of concentrations (mM). After 18 h incubation, pellicle and surface-adherent (SA) biofilm formation were evaluated. The values (mode of at least three independent experiments each performed in triplicate) indicate the break-point concentration: that which resulted in the loss of biofilm formation (A) or most dramatic difference in morphology (B). ND, not done.

Discussion

Array analysis predicts that acP mediates biofilm initiation

DNA macroarray experiments designed specifically to identify acP target genes provide evidence that acP (i) positively regulates genes required for type 1 pilus assembly, colanic acid biosynthesis and protection against certain stresses and (ii) negatively regulates genes required for flagella assembly (see also Prüß and Wolfe, 1994). Each of these acP-responsive structures or processes contributes to pellicle or surface-adherent biofilm formation, developmental programmes that require these structures and processes to be available in the proper amount and in the appropriate order (Stoodley *et al*., 2002). We therefore tested whether mutants defective in their ability to metabolize acP could construct normal biofilms, and found that they could not.

acP metabolism mutants form aberrant biofilms

Both the *ackA* mutant that accumulates acP and the *pta ackA* mutant that cannot synthesize acP clearly form biofilms; however, these biofilms exhibit morphological and physical properties distinctly different from each other and their wild-type parent. Whereas the *ackA* mutant forms a poor surface-adherent biofilm composed of small microcolonies and a pellicle composed of isolated colony-like structures, the *pta ackA* mutant forms a more abundant surface-adherent biofilm and a rather featureless, film-like pellicle. Intriguingly, wild-type cells form pellicles that appear to incorporate both characteristics: *ackA*-like structures that sit upon a *pta ackA*-like film. Whereas the *pta ackA* mutant pellicle disperses easily upon agitation, the wild-type and *ackA* mutant biofilms resist dispersal. This makes sense, as type 1 pili contribute to cell–cell contact, *pta ackA* mutants appear to be defective in pilus assembly, and inhibition of the mannose-specific FimH

adhesin exerts no great influence upon the formation of *pta ackA* mutant biofilms. However, pili must contribute to some degree, because their complete absence or simply that of FimH completely eliminates *pta ackA* mutant biofilm formation. In contrast, flagella clearly play a key role in the formation of biofilms by the hyperflagellated *pta ackA* cells and apparently an insignificant role in biofilm formation by the already poorly flagellated *ackA* cells. Taken together, these results suggest that *pta ackA* and *ackA* mutants form aberrant biofilms via somewhat different developmental pathways that rely to varying degrees upon structures (i.e. type 1 pili and flagella), the expression of which appears to be responsive to the status of the acP pool. In contrast, wild-type biofilm formation depends on all three structures (Stoodley *et al*., 2002).

acP as a signal of nutritional status

What causes the *pta ackA* and *ackA* mutants to synthesize flagella, type 1 pili and capsule differently enough to construct biofilms with distinctly different attributes? The characteristic phenotypes of both mutants did not vary under a number of laboratory conditions. For example, both mutants exhibit their characteristic phenotypes when grown in either TB or LB at either 37°C or 30°C (J. E. Seitz-Partridge and A. J. Wolfe, unpublished). When backcrossed to its wild-type parent, each mutant exhibits its characteristic behaviour (J. E. Seitz-Partridge and A. J. Wolfe, unpublished). These observations argue against a role for a temperature-sensitive structure or process or some unknown, uncharacterized mutation that might be influenced by media composition. Both mutants cannot recycle CoASH by the preferred method (i.e. the Pta-AckA pathway), both excrete little or no acetate, and both only modestly acidify their environment before evolving large amounts of ammonia (B. M. Prüß and A. J. Wolfe, unpublished). Thus, we must look elsewhere for the underlying cause of the mutants' morphological and physical properties. The status of their acP pool stands out as the most obvious difference between the two mutants: whereas *pta ackA* mutants cannot synthesize acP, *ackA* mutants accumulate it in excess (McCleary and Stock, 1994; Prüß and Wolfe, 1994).

Its central role in intermediary carbon metabolism positions acP suitably to monitor nutritional status. The acP pool rises rapidly during exponential growth in an aerated culture replete with nutrients; the pool falls as the cells deplete those nutrients and begin their transition to stationary phase (Prüß and Wolfe, 1994). Direct measurement of acP in cells that have entered stationary phase provides evidence that the acP pool rises again after cells enter stationary phase (McCleary and Stock, 1994). This increase during stationary phase may occur in response to starvation and/or the lack of oxygen. The glucose starvation response, which includes increased levels of Pta and decreased levels of TCA cycle enzymes, depends upon Pta but not AckA, an observation that argues that acP helps to induce that response (Nystrom, 1994), presumably via ArcA, a two-component response regulator (Nystrom *et al*., 1996). A similar response occurs as cells transit from aerobic to anaerobic conditions that result in fermentation (Nystrom, 1994). Thus, it appears that acP concentrations rise in the absence of a functional TCA cycle, e.g. during starvation or fermentation, or whenever the accumulation of acCoA exceeds the TCA cycle's capacity, e.g. during rapid growth. In contrast, the acP pool diminishes whenever the acCoA pool does not exceed its capacity, e.g. during the transition from exponential growth to stationary phase.

acP as a modulator of biofilm development

These reported observations pertain to cells aerated in shake flask cultures. However, we have reason to believe that a similar sequence of events occurs during growth in static culture. First and foremost, in both aerated and static culture, *pta ackA* and *ackA* mutant cells exhibit strikingly similar growth, amino acid consumption and ammonia evolution profiles. Secondly, initiation of wild-type biofilm formation occurs before 6 h (Fig. 6B), an interval that coincides with the beginning of the transition phase. Assuming that wild-type cells grown in static culture co-ordinate metabolic and physiological events similarly to those grown in aerated culture, we expect that the acP pool decreases and flagella expression increases during the interval just before the transition phase. Later, as the local extracellular environment becomes increasingly anaerobic and depleted of nutrients, we predict that the acP pool increases with a concomitant increase in type 1 pilus and colanic acid biosynthesis. Thus, acP could serve as a signal to initiate pellicle and surface-adherent biofilm formation by modulating an orderly switch between the flagella-dependent, the pili-dependent and the capsule-dependent stages of biofilm formation, as has been established for wild-type biofilm development (Stoodley *et al*., 2002).

acP as a phosphodonor for response regulators

acP can act as a phosphodonor for some response regulators (McCleary *et al*., 1993; Wanner, 1995). Thus, we find it tempting to hypothesize that acP influences biofilm formation by acting as a phosphodonor for response regulators (FimZ, OmpR and RcsB) that control certain biofilm-associated genes. Phospho-FimZ and phospho-OmpR repress flagellar synthesis (Shin and Park, 1995; Clegg and Hughes, 2002), whereas phospho-FimZ activates type 1 pilus expression (Clegg and Hughes, 2002).

Phospho-RcsB activates colanic acid biosynthesis (Stout, 1994) and at least one acP-responsive stress effector (*osmC*) (Davalos-Garcia *et al*., 2001).

Implications for biofilm development in the wild type

The results of DNA macroarray experiments designed to identify acP-responsive genes argue that the status of the acP pool modulates the expression of cellular components required for the normal development of biofilms. We envisage that acP modulates the initial steps of biofilm formation by linking the expression of flagella, pili and colanic acid to the nutritional status of the culture, presumably by means of several two-component response regulators. We expect that wild-type planktonic cells, experiencing the transition from exponential growth to stationary phase, possess a small acP pool, assemble several flagella and some pili and synthesize little colanic acid. Once these wild-type cells make contact with a suitable surface or with each other, however, we predict that the subsequent local depletion of nutrients and oxygen will cause intracellular acP levels to rise. In response, flagella synthesis will diminish, and first pili and then colanic acid biosynthesis will increase. Clearly, the dynamic relationships between nutritional environment, acP pool, acP-responsive signal transduction pathways and the targets of those pathways warrant further study.

Experimental procedures

Bacterial strains

All strains used in this study were derivatives of *E. coli* K-12 and are listed in Table 5.

Culture conditions

Cells were grown aerobically with 250 r.p.m. agitation at 37°C in tryptone broth [TB; 1% (w/v) tryptone and 0.5% (w/v) sodium chloride] in 250 ml fleakers (Corning). Cell growth was monitored spectrophotometrically (Beckman Instruments DU530) at 590 nm (A590) by removing 100 μl samples without interrupting culture agitation; no more than 5% of the culture was removed before harvesting cells for RNA isolation. Cultures were inoculated to an initial A_{590} of <0.001 to ensure that the cells experienced at least 10 generations in the medium before reaching steady-state growth.

Amino acid analysis

Amino acid analysis of culture media was performed as described previously (Prüß *et al*., 1994).

RNA isolation

Cells for RNA isolation were harvested from the early exponential phase of growth; 10 ml of culture was pipetted into 10 ml of ice-cold RNA-Later (Ambion). Cells were removed from this mixture by centrifugation (8730 *g* for 20 min). RNA was isolated and purified using an RNeasy mini kit (Qiagen). Genomic DNA was removed after purification by DNase I (Ambion) treatment, with subsequent RNA repurification with an RNeasy column. RNA samples were quantified by 260 nm absorbance (Beckman DU530 spectrophotometer).

Labelled target synthesis

Labelled targets for hybridization were generated as described previously (Tao *et al*., 1999) with slight modifications. The initial preincubation (90°C for 2 min, then 42°C for 20 min in an MJ Research MiniCycler) was performed in 0.2 ml PCR tubes containing 1 μg of RNA template, dATP, dCTP and dGTP (0.33 mM each final concentration) and C-

Table 5. Bacterial strains used in this study.

Strain	Relevant genotype	Source or reference
AJW678	*thi-1 thr-1*(Am) *leuB6 metF159*(Am) *rpsL136* Δ*lacX74*	Kumari *et al*. (2000)
AJW1939	AJW678 *ackA*::Km	Kumari *et al*. (2000)
AJW2067	AJW678 *ackA*::Tn*phoA′-2*	(P1)CP757→AJW678 (Tc/Ace–)
AJW2013	AJW678 Δ(*ackA pta hisJ hisP dhu*) *zej223*-Tn*10*	(P1)CP911→AJW678 (Tc/Ace–)
AJW2061	AJW678 *fimH*::Km	(P1)ORN133→AJW678 (Km)
AJW2069	AJW678 *ackA*::Tn*phoA′-2 fimH*::Km	(P1)ORN133→AJW2067 (Km)
AJW2062	AJW678 Δ(*ackA pta hisJ hisP dhu*) *zej223*-Tn*10 fimH*::Km	(P1)ORN133→AJW2013 (Km)
AJW2063	AJW678 Δ*fimA*::Km	(P1)ORN172→AJW678 (Km)
AJW2070	AJW678 *ackA*::Tn*phoA′-2* Δ*fimA*::Km	(P1)ORN172→AJW2067 (Km)
AJW2064	AJW678 Δ(*ackA pta hisJ hisP dhu*) *zej223*-Tn*10* Δ*fimA*::Km	(P1)ORN172→AJW2013 (Km)
AJW2145	AJW678 *fliA*::Tn*5*	(P1)MG1665 *fliA::*Tn*5*→AJW678 (Km)
AJW2149	AJW678 *ackA*::Km *fliA*::Tn*5*	(P1)AJW2145→AJW1939 (Km)
AJW2153	AJW678 Δ(*ackA pta hisJ hisP dhu*) *zej223*-Tn*10 fliA*::Tn*5*	(P1)AJW2145→AJW2013 (Km)
CP750	*thi-1 thr-1*(Am) *leuB6 metF159*(Am) *rpsL136*	Shin and Park (1995)
CP757	CP750 *ackA*::Tn*phoA′-2*	C. Park (KAIST, Korea)
CP911	CP750 Δ(*ackA pta hisJ hisP dhu*) *zej223*-Tn*10*	Prüß *et al*. (1994)
MG1655 *fliA::*Tn*5*	*fliA*::Tn*5*	F. Blattner (University of Wisconsin, Madison, WI, USA)
ORN133	*fimH*::Km	P. Orndorff (North Carolina State University)
ORN172	Δ*fimA*::Km	P. Orndorff

terminal primers (Sigma Genosys Biotechnologies) brought to a final volume of 23 μl with RNase-free dH_2O. After preincubation, a labelling mix {20 μCi [α-^{33}P]-dCTP (2000–3000 Ci mol^{-1}, New England Nuclear), 200 units of Superscript II RNase H$^-$ reverse transcriptase (BRL), 10 mM dithiothreitol (DTT; BRL) and 10 units of ribonuclease inhibitor (BRL)} was added, bringing the final volume to 30 μl. The cDNA reaction mixture was incubated for 2 h at 42°C. The labelled cDNA was denatured from the RNA template for 30 min at 65°C with 29 mM EDTA and 0.43 N NaOH. The denaturing reaction was neutralized with 160 mM Tris (pH 7.4) and 0.28 N HCl. The amount of radiolabel incorporation during labelling was determined by comparing scintillation counts of 1 μl of labelled cDNA (in 5.0 ml of scintillation fluid) before and after removal of unincorporated nucleotide by gel filtration through a G-50 Sephadex column (Sambrook *et al*., 1989). This procedure routinely supplied cDNA samples with 70–90% label incorporation.

Hybridization of arrays and image analysis

Panorama *E. coli* gene arrays (Sigma Genosys Biotechnologies), array prehybridization, hybridization and array washes were performed as described previously (Tao *et al*., 1999), with the following modifications. Before prehybridization, arrays were rinsed in 50 ml of 2× SSPE (1× SSPE is 0.18 M NaCl, 10 mM NaH_2PO_4 and 1 mM EDTA, pH 7.7), then prehybridized with 5 ml of hybridization solution (65°C for 1–4 h) and hybridized with 3.0 ml of hybridization solution supplemented with 400–600 μl of labelled cDNA probe (65°C for 16–18 h). The arrays were then wrapped in clear plastic food wrap (Saran Wrap) and exposed to a Kodak storage phosphor screen GP (Eastman Kodak) for 24 h. Longer exposure times were occasionally necessary to increase spot visibility and contrast. Exposed phosphor screens were visualized at a pixel density of 100 microns (10 000 dots cm^{-2}) with a Storm 820 PhosphorImager (Molecular Dynamics). The array membranes were consecutively hybridized, stripped and rehybridized, a procedure that was repeated up to eight times. Arrays were stripped of hybridized probe by boiling the inverted array for 20 min in a microwave (100°C) in 200 ml of stripping solution (10 mM Tris, pH 7.5, 1 mM EDTA and 1% SDS). Phosphorimaging of a membrane array results in a TIFF image file that was processed for data analysis, as described previously (Conway *et al*., 2002). The raw spot intensities were represented in a row–column format and exported into Microsoft EXCEL spreadsheets for further analysis.

Data analysis

The level of replication used in this study has been shown to provide robust statistical analysis and minimizes false positives (Conway *et al*., 2002). The raw data from each experimental replicate were exported to EXCEL workbooks and processed as described previously (Conway *et al*., 2002). The duplicate spots on the arrays were treated as separate determinations. The raw data values were normalized by expressing each gene as a percentage of the sum of all the gene-specific spot intensities. The probability that the average of the experimental replicates is significantly different from the average of the control replicates was calculated by application of Student's *t*-test. The ratio of the experimental/control expression levels was calculated such that genes that are more highly expressed in the experimental condition are given a positive value and genes that are more highly expressed in the control condition are given a negative value. Statistical significance is established by consideration of two metrics, the *P*-value, which takes into consideration the uncertainty of the replicate measurements for both conditions, and the standard deviation of the mean of the log (base 10) ratios, which indicates the significance of the ratio. For consideration of genes affected by mutations resulting in altered intracellular concentrations of acP, we considered only those genes that were significantly up- or downregulated by >2.5 standard deviations from the mean of the log ratios (99% confidence) with *P*-values ≤0.05 (95% probability).

Website and public access to analysis tools

A website has been constructed to permit users to download these analytical tools and protocols that describe their step-by-step implementation (http://www.ou.edu/microarray).

Quantitative RT-PCR

Real-time PCR was performed with RNA samples, prepared as described above. RNA was reverse transcribed using amino-allyl reverse transcription (http://www.cmgm.stanford.edu/pbrown/protocols/aadUTPCouplingProcedure.htm), and cDNA was purified. The PCR was performed with the SYBR green kit from PE Biosystems. The reaction mixture contained 100 ng of cDNA, 1× SYBR green buffer, 2.5 mM $MgCl_2$, 0.25 mM each dNTP, 0.05 μM each primer, 0.01 U of AmpErase UNG and 1 U of *Taq* Gold polymerase. The reaction was performed with 50 cycles of 30 s at 94°C, 30 s at 55°C and 1 min at 72°C and monitored in an iCycler iQ real-time PCR detection system (Bio-Rad). A standard curve was derived from plasmid and used to convert threshold crossings to log copy numbers. Expression ratios were obtained by dividing copy numbers of wild-type cells by those of the mutants. All PCR fragments yielded a single band on agarose gel.

Biofilm and pellicle techniques

Cell growth was monitored spectrophotometrically (Beckman Instruments DU530) at A_{590}. Cells were grown in microtitre wells without aeration at 37°C in TB. At 2 h intervals, the entire well was harvested. To ensure that all cells were harvested, the well was rinsed three times with fresh media. To ensure a homogeneous suspension, the cells were passed through a small bore tube connected at both ends to a syringe. Surface-adherent biofilms were stained with crystal violet as described previously (Pratt and Kolter, 1998) and visualized using an Alphaimager 2000 documentation and analysis system. Pellicles were photographed before harvesting, using a Wild (Heerbrugg) dissecting microscope.

Microscopic techniques

Light microscopy. Glass strips cut from sterile microscope

slides were suspended in static culture tubes containing 3 ml of TB so that the waterline bisected the strips. The tubes were inoculated and, at intervals during growth, strips were removed and examined along their length using a Nikon Microphot light microscope with differential interference contrast optics. Digital images were captured with a Spot RT digital camera.

Transmission electron microscopy. Cells were grown in TB with aeration at 37°C to an A_{590} = 0.4. Whole cells placed on collodion-coated copper grids were negative stained by brief treatment with 2% uranyl acetate. Grids were observed and photographed on a Jeol 100CX transmission electron microscope.

Acknowledgements

We thank K. Visick, A. Driks, T. Gallagher and P. Orndorff for their advice and insight, and F. Blattner and P. Orndorff for strains. This work was supported by grants MCB-9630647 from the National Science Foundation and LU#11200 from the Loyola University Chicago Potts Foundation (A.J.W.) and grant RO1-AI-48945-01 from the NIH (T.C.).

Supplementary material

The following material is available from http://www.blackwellpublishing.com/products/journals/suppmat/mole/mole3457/mmi3457sm.htm

Table S1. Genes significantly upregulated in a *pta ackA* mutant compared to an *ackA* mutant.

Table S2. Genes significantly upregulated in an *ackA* mutant compared to a *pta ackA* mutant.

Table S3. Genes significantly upregulated in both mutants compared to wild type.

Table S4. Genes significantly downregulated in both mutants compared to wild type.

Fig. S1. A. A_{590} for wild-type cells (AJW678; □), or deficient for either *ackA* (AJW1939; ○) or *pta ackA* (AJW2013; △). Cells were grown without aeration at 37°C in TB.

B. Amino acid concentrations in the medium of cells deficient for *ackA* (AJW1939) or (C) for *pta ackA* (AJW2013). (▲) L-serine, (■) L-aspartate, (▽) L-tryptophan, (□) L-glycine, (▼) L-glutamate, (●) L-threonine, (○) L-alanine. Amino acids that did not change significantly are not shown.

D. Ammonia concentrations in the medium of cells defective for *ackA* (AJW1939) (○) and *pta ackA* (AJW2013) (△). Each point represents the mean of duplicate measurements from two independent experiments. The standard errors of the means were less than 20 μmoles l^{-1}.

References

Barker, M.M., Gaal, T., Josaitis, C.A., and Gourse, R.L. (2001a) Mechanism of regulation of transcription initiation by ppGpp. I. Effects of ppGpp on transcription initiation *in vivo* and *in vitro*. *J Mol Biol* **305:** 673–688.

Barker, M.M., Gaal, T., and Gourse, R.L. (2001b) Mechanism of regulation of transcription initiation by ppGpp. II. Models for positive control based on properties of RNAP mutants and competition for RNAP. *J Mol Biol* **305:** 689–702.

Brown, T.D.K., Jones-Mortimer, M.C., and Kornberg, H.L. (1977) The enzymic interconversion of acetate and acetyl-coenzyme A in *Escherichia coli*. *J Gen Microbiol* **102:** 327–336.

Bruckner, R., and Titgemeyer, F. (2002) Carbon catabolite repression in bacteria: choice of the carbon source and autoregulatory limitation of sugar utilization. *FEMS Microbiol Lett* **209:** 141–148.

Chang, D.-E., Shin, S., Rhee, J.-S., and Pan, J.-G. (1999) Acetate metabolism in a *pta* mutant of *Escherichia coli* W3110: importance of maintaining acetyl-CoA flux for the growth and survival. *J Bacteriol* **181:** 6656–6663.

Chang, D.-E., Smalley, D., and Conway, T. (2002) Gene expression profiling of *Escherichia coli* growth transitions: an expanded stringent response model. *Mol Microbiol* **45:** 289–306.

Clegg, S., and Hughes, K.T. (2002) FimZ is a molecular link between sticking and swimming in *Salmonella enterica* serovar Typhimurium. *J Bacteriol* **184:** 1209–1213.

Conway, T., Kraus, B., Tucker, D.L., Smalley, D.J., Dorman, A.F., and McKibben, L. (2002) DNA array analysis in a Microsoft windows environment. *Biotechniques* **32:** 110–119.

Danese, P.N., Pratt, L.A., and Kolter, R. (2001) Biofilm formation as a developmental process. *Methods Enzymol* **336:** 19–26.

Davalos-Garcia, M., Conter, A., Toesca, I., Gutierrez, C., and Cam, K. (2001) Regulation of *osmC* gene expression by the two-component system *rcsB-rcsC* in *Escherichia coli*. *J Bacteriol* **183:** 5870–5876.

Harris, S.L., Elliott, D.A., Blake, M.C., Must, L.M., Messenger, M., and Orndorff, P.E. (1990) Isolation and characterization of mutants with lesions affecting pellicle formation and erythrocyte agglutination by type 1 piliated *Escherichia coli*. *J Bacteriol* **172:** 6411–6418.

Hung, S.P., Baldi, P., and Hatfield, G.W. (2002) Global gene expression profiling in *Escherichia coli* K12: the effects of leucine-responsive regulatory protein. *J Biol Chem* **277:** 40309–40323.

Kumari, S., Beatty, C.M., Browning, D.F., Busby, S.J., Simel, E.J., Hovel-Miner, G., and Wolfe, A.J. (2000) Regulation of acetyl coenzyme A synthetase in *Escherichia coli*. *J Bacteriol* **182:** 4173–4179.

McCleary, W.R., and Stock, J.B. (1994) Acetyl phosphate and the activation of two-component response regulators. *J Biol Chem* **269:** 31567–31572.

McCleary, W.R., Stock, J.B., and Ninfa, A.J. (1993) Is acetyl phosphate a global signal in *Escherichia coli*? *J Bacteriol* **175:** 2793–2798.

el-Mansi, E.M., and Holms, W.H. (1989) Control of carbon flux to acetate excretion during growth of *Escherichia coli* batch and continuous cultures. *J Gen Microbiol* **135:** 2875–2883.

Nystrom, T. (1994) The glucose-starvation stimulon of

Escherichia coli: induced and repressed synthesis of enzymes of central metabolic pathways and role of acetyl phosphate in gene expression and starvation survival. *Mol Microbiol* **12:** 833–843.

Nystrom, T., Larsson, C., and Gustafsson, L. (1996) Bacterial defense against aging: role of the *Escherichia coli* ArcA regulator in gene expression, readjusted energy flux and survival during stasis. *EMBO J* **15:** 3219–3228.

Pratt, L.A., and Kolter, R. (1998) Genetic analysis of *Escherichia coli* biofilm formation: roles of flagella, motility, chemotaxis and type I pili. *Mol Microbiol* **30:** 285–293.

Prüß, B.M., and Wolfe, A.J. (1994) Regulation of acetyl phosphate synthesis and degradation, and the control of flagellar expression in *Escherichia coli*. *Mol Microbiol* **12:** 973–984.

Prüß, B.M., Nelms, J.M., Park, C., and Wolfe, A.J. (1994) Mutations in NADH: ubiquinone oxidoreductase of *Escherichia coli* affect growth on mixed amino acids. *J Bacteriol* **176:** 2143–2150.

Rose, I.A., Grunsberg-Manago, M., Korey, S.R., and Ochoa, S. (1954) Enzymatic phosphorylation of acetate. *J Biol Chem* **211:** 737–756.

Sambrook, J., Fritsch, E.F., and Maniatis, T. (1989) *Molecular Cloning: A Molecular Laboratory Manual*. Cold Spring Harbor, NY: Cold Spring Harbor Laboratory Press.

Sauer, F.G., Barnhart, M., Choudhury, D., Knight, S.D., Waksman, G., and Hultgren, S.J. (2000) Chaperone-assisted pilus assembly and bacterial attachment. *Curr Opin Struct Biol* **10:** 548–556.

Shin, S., and Park, C. (1995) Modulation of flagellar expression in *Escherichia coli* by acetyl phosphate and the osmoregulator OmpR. *J Bacteriol* **177:** 4696–4702.

Stoodley, P., Sauer, K., Davies, D.G., and Costerton, J.W. (2002) Biofilms as complex differentiated communities. *Annu Rev Microbiol* **56:** 187–209.

Stout, V. (1994) Regulation of capsule synthesis includes interactions of the RcsC/RcsB regulatory pair. *Res Microbiol* **145:** 389–392.

Tao, H., Bausch, C., Richmond, C., Blattner, F.R., and Conway, T. (1999) Functional genomics: expression analysis of *Escherichia coli* growing on minimal and rich media. *J Bacteriol* **181:** 6425–6440.

Wanner, B.L. (1995) Signal transduction and cross regulation in the *Escherichia coli* phosphate regulon by PhoR, CreC, and acetylphosphate. In *Two Component Signal Transduction.* Hoch, J.A., and Silhavy, T.J. (eds). Washington, DC: American Society for Microbiology Press, pp. 203–221.

Wanner, B.L., and Wilmes-Riesenberg, M.R. (1992) Involvement of phosphotransacetylase, acetate kinase, and acetyl phosphate synthesis in control of the phosphate regulon in *Escherichia coli*. *J Bacteriol* **174:** 2124–2130.